



Structural, Morphological, Thermal and Mechanical Study of a Geopolymer Based on Metakaolin Mixed with Oujda Clay [†]

Youssef Bachirat, Assaad Elouafi *  and Abdeslam Tizliouine 

LMPGI, Higher School of Technology, Hassan II University of Casablanca, Casablanca 8012, Morocco

* Correspondence: assaadelouafi@gmail.com[†] Presented at the 3rd International Electronic Conference on Processes—Green and Sustainable Process Engineering and Process Systems Engineering (ECP 2024), 29–31 May 2024; Available online: <https://sciforum.net/event/ECP2024>.

Abstract: This study investigated a metakaolin-based geopolymer blended with Oujda clay, replacing 5–15 wt% of metakaolin (MK) and is focused on structural, thermal stability, and microstructural changes in the geopolymer pre- and post-high temperature exposure, using XRD, TGA, FTIR, and SEM. Results showed that Oujda clay addition increased compressive strength to 33 MPa with 15 wt% clay after 28 days of curing. To facilitate the replacement of metakaolin-based geopolymer, the amount of metakaolin was decreased by incorporating Oujda clay. This strategy enabled chemical and mechanical properties comparable to those of traditional metakaolin-based geopolymer, while also introducing a more locally sourced and potentially cost-effective material.

Keywords: geopolymer; Oujda clay; morphology; mechanical properties; microcracks; protective layer

1. Introduction

Clay is widely found globally and is commonly encountered in road and railway construction in Morocco. The weak microstructure bonding of clay particles makes superstructures vulnerable to significant damage such as cracking, subsidence, and collapse [1]. A geopolymer is created by mixing mineral materials with strong alkaline solutions to produce a three-dimensional, amorphous aluminosilicate network [2]. This process dissolves and rearranges aluminosilicate, forming oligomers that link large polymers together [3]. Geopolymers made from calcined materials like metakaolin (MK) are known for their high strength [4]. The crystal and chemical structures of natural minerals vary based on how silica and alumino interact with alkaline solutions [5]. Amorphous geopolymers form at condensation temperatures between 20 and 90 °C, while crystalline geopolymers are produced at 150–200 °C [6,7]. Typically, geopolymers are heat-cured for 2–72 h [8,9]. Unlike calcium–silicate–hydrate gels, geopolymers gain their strength through the polycondensation of silica and alumino precursors [9]. MK stands out as it is a natural material derived from the calcination of kaolin, hydrated aluminosilicate clay, not a byproduct of industrial processes [4]. MK is a high-performance material with a high SiO₂ and Al₂O₃ content, produced by sintering kaolin clay at 600–900 °C. Geopolymers made from MK typically have a Si:Al ratio between 0.5 and 3.0, but a higher Si:Al ratio requires increased sodium content, which can be achieved with sodium hydroxide [10]. Geopolymers made from MK and slag offer the highest strength and durability, with notable compressive strength achieved early in the curing process [11,12]. Several pieces of research have been carried out in this area. Lecomte et al. [13] indicated that both normal and separate mixing (alumino–silicate with an alkali silicate solution) methods maintain the degree of geopolymerization in kaolin/white clay-slag geopolymers. However, separate mixing requires additional water, which can weaken mechanical strength. In contrast, Rattanasak and Chindaprasirt [14] found that separate mixing for fly ash geopolymers allows more time for aluminosilicate dissolution, enhancing the polycondensation process and resulting



Citation: Bachirat, Y.; Elouafi, A.; Tizliouine, A. Structural, Morphological, Thermal and Mechanical Study of a Geopolymer Based on Metakaolin Mixed with Oujda Clay. *Eng. Proc.* **2024**, *67*, 43. <https://doi.org/10.3390/engproc2024067043>

Academic Editor: Juan Francisco García Martín

Published: 14 September 2024



Copyright: © 2024 by the authors. Licensee MDPI, Basel, Switzerland. This article is an open access article distributed under the terms and conditions of the Creative Commons Attribution (CC BY) license (<https://creativecommons.org/licenses/by/4.0/>).

in stronger geopolymers. Achieving homogeneity in geopolymer mixtures is crucial for attaining high strength. Workability is essential in geopolymer formation; poor workability leads to compaction issues and weak structures [15,16]. Clay-based geopolymers often require extra water for the right consistency, which decreases their mechanical strength. Compared to fly ash geopolymers, clay-based mixtures are more viscous and stickier due to clay's layered structure and high inter-particle friction. Fly ash's spherical particles reduce friction, achieving adequate consistency without extra water [17]. Geopolymers are widely used in engineering, primarily for partial replacement of cement mortar and concrete, with fewer applications in soil stabilization [18]. Xiang's study on fly ash-stabilized loess shows that decreasing the modulus of water glass and increasing the Baume degree significantly enhances the compressive strength of loess stabilized with fly ash-based cementing material [19]. In this study, the structural, morphological, thermal and mechanical properties of a geopolymer based on metakaolin mixed with Oujda clay were investigated.

2. Experimental Section

Completely calcined Oujda clay with high chemical reactivity (treated with 8 M NaOH) and low crystalline SiO₂ content can be prepared by controlling the calcination temperature at 700 °C, with a heating rate of 5 °C/min and a holding time of 4 h. Metakaolin (MK) was provided by SOKA (Armorican Kaoliner Society) in France. The Oujda clay was supplied by the agricultural sector in Oujda, Morocco. To obtain a homogeneous particle size, a 56 µm sieve was used for metakaolin and a 67 µm sieve for Oujda clay. The metakaolin-based geopolymer mixed with Oujda clay was used in a 50% water-saturated state. The aim was to examine the change in geopolymers with changing material weight ratios, keeping the water ratio constant. The alkali activator used in this study was a combination of sodium silicate solution and sodium hydroxide (96% NaOH). The liquid components in the mixture included 8M sodium hydroxide (NaOH) and sodium silicate (Na₂SiO₃), which consisted of 8.2% Na₂O, 26.0% SiO₂, and 56.6% H₂O. The alkali activator solution was premixed and allowed to rest for 24 h at ambient temperature before casting. Figure 1 shows Oujda clay powder before and after chemical treatment.

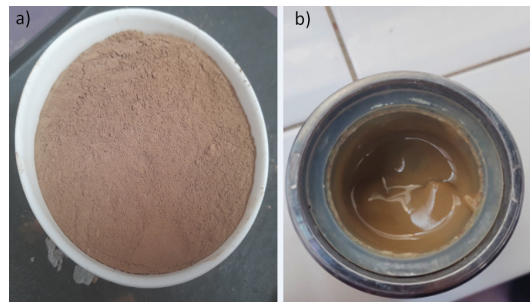


Figure 1. (a) Oujda clay powder; (b) chemical treatment of Oujda clay powder with NaOH.

As shown in Figure 2, three series of geopolymer samples were synthesized by mixing alkali activation of MK and Oujda clay in alkali-silicate solutions (modulus of alkaline activator MR = 1.5).

Oujda clay and Metakaolin (MK) were mixed with alkali solutions for 5 min. Fresh geopolymer pastes were poured in rectangular molds with a size of 4 × 4 × 16 cm³. All samples were cured at room temperature for 24 h and further cured in a standard curing chamber (25 ± 2 °C and 95 ± 2% relative humidity (RH)) for 7 and 28 days. Metakaolin-based geopolymer (MKG) and Metakaolin based geopolymer blended with Oujda clay with the highest compressive strength were selected as thermal stability experimental groups. Chemical compositions of MK and Oujda clay analyzed by Fluorescence X-ray analysis (XRF) are listed in Table 1. It is evident from Table 1 that the precursors are composed of a high content of silicate and aluminate. The silicate content of MK and Oujda clay is 55% and 38%, respectively, while the corresponding aluminate content is 39% and 12.65%,

respectively. The high content of these monomers (i.e., silicate and aluminate) in these materials makes them a suitable candidate for the production of geopolymer binders. The silicate to aluminate ratio (Si:Al) is known to influence the geopolymerization reaction.

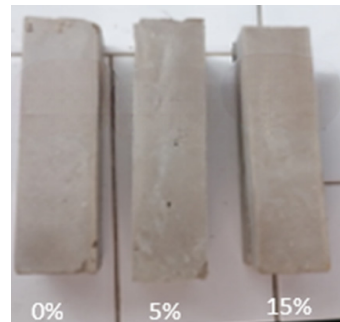


Figure 2. Different geopolymer alkali-activated prismatic samples with different percentage of Oujda clay.

Table 1. Chemical composition of Metakaolin and Oujda clay.

Composition of Metakaolin M1200S	SiO ₂	Al ₂ O ₃	K ₂ O	Fe ₂ O ₃	MgO	TiO ₂
Proportion (%)	55.00	39.00	1.2	0.6	0.2	0.5
Composition for Oujda clay	SiO ₂	Al ₂ O ₃	K ₂ O	Fe ₂ O ₃	ZnO	CaO
Proportion (%)	38.4	12.65	1.67	11.9	2.96	28.9

Several techniques were used to study the different characteristics of the samples, including Fourier Transform Infrared spectroscopy (FTIR) (IR affinity-1S Shimadzu, Kyoto, Japan), X-ray diffraction (XRD) (Bruker D8 Advance, CuK_{α1}, λ = 1.540598 Å, Karlsruhe, Germany), scanning electron microscopy (SEM) (FEI FEG 450, Hillsboro, OH, USA) and thermogravimetric analysis (SUMILTANEOU TG/DTA, Kyoto, Japan). Mechanical behavior of the prepared geopolymer samples was assessed by compression tests (Figure 3).

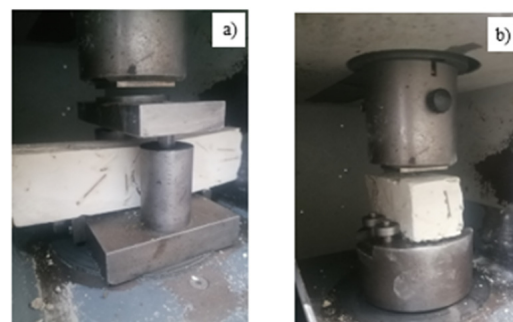


Figure 3. (a) Flexural test; (b) compressive test of geopolymer based on fiber at 28 days.

3. Results and Discussions

3.1. X-ray Diffraction Analysis

Figure 4 presents the XRD analysis of geopolymer pastes containing various levels of Oujda clay replacement. An amorphous glassy phase is noticeable in all samples within the 25°–40° range of 2θ angles. This halo indicates the formation of an alkaline aluminosilicate gel (N–A–S–H gel), which is the primary product generated during the geopolymerization process [20,21]. XRD plots show peaks of crystalline phases corresponding to illite, quartz, hematite, and anatase [22]. The peaks around 30.19°, 35.68°, 39.42° and 41.3° 2θ in the patterns generally indicate sodium. The crystalline and semicrystalline phases were detected within a range of 20° to 30° of 2θ, indicating the presence of calcium silicate hydrate (C–S–H). All ternary blended geopolymer samples were cured under ambient conditions and exhibited identical crystalline phases, including quartz (2θ = 26.67; Q as

per JCPDS Number 88-2488), calcium magnesium silicate ($2\theta = 28.04$; C-M-S as per JCPDS Number 84-1743) and calcium silicate hydrate ($2\theta = 28.043$; C-S-H as per the JCPDS Number).

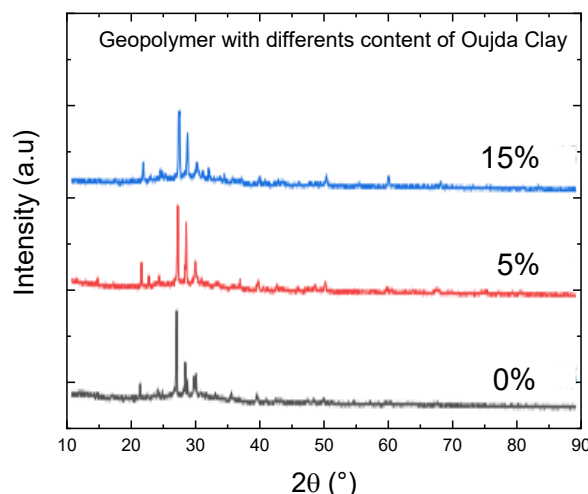


Figure 4. XRD diffractograms of geopolymers synthesized with various contents of Oujda Clay.

3.2. Scanning Electron Microscopy (SEM)

Figure 5 illustrates the microstructures of MK and Oujda clay. Metakaolin (MK) contains an amorphous phase predominantly composed of metakaolinite. In contrast, Oujda clay includes a variety of hardly soluble crystals such as Quartz, Kaolinite, Kyanite, and Muscovite. Particle size distribution is very similar between MK and Oujda clay. MK exhibits a layered amorphous aluminosilicate structure with an irregular molecular arrangement [23]. It is in a thermodynamically metastable state with high pozzolanic activity and exhibits gelling properties when appropriately activated. Other studies [24,25] have found that the proportion of Si to Na or K atoms in the alkali silicate solution influences the extent of polymerization of the dissolved elements. The dense structure is characterized by the dissolution of alkali-activated Al^{3+} , Si^{4+} , and Ca^{2+} . On the other hand, Oujda clay displays a loose and porous, thin-walled structure with its inner surface covered by a layer of nano-silica microspheres (~100 nm). This clay exhibits exceptional chemical reactivity owing to its large specific surface area and the presence of nano-scale reactive sites on its inner surface [26].

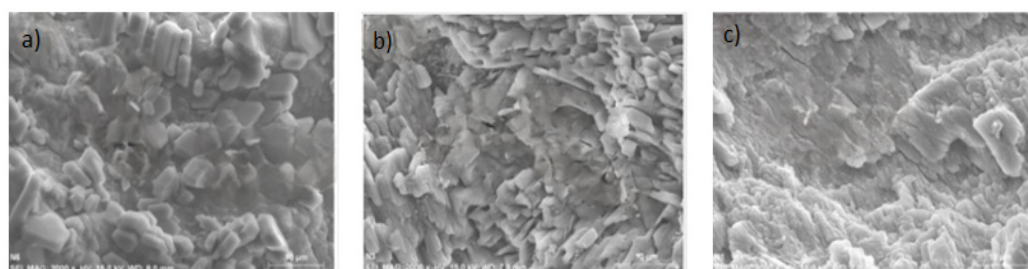


Figure 5. SEM analysis of MK with various contents of Oujda clay; (a):0%; (b): 5%; (c): 15%.

3.3. FTIR Analysis

Figure 6 displays the FTIR spectra ($400\text{--}4000\text{ cm}^{-1}$) of MGK cured for 28 days with 15% Oujda clay. The absorption band at 471 cm^{-1} is associated with the Si–O–Si in-plane bending vibration, while the band at 727 cm^{-1} is attributed to the symmetric stretching vibration of Si–O bonds [27,28]. Following the reaction between silicon aluminates and the alkali solution, the geopolymer structure involves bending vibrations of Si–O–Al bonds between the 471 cm^{-1} and 729 cm^{-1} bands. Absorption bands between 1448 cm^{-1} and

1642 cm^{-1} correspond to the stretching vibrations of O–H groups in water molecules. Additionally, a peak at 1448 cm^{-1} indicates the presence of C*O vibration, suggesting carbonation of the geopolymer. This phenomenon is due to the decomposition of the activator Na_2CO_3 into Na_2O and CO_2 [29].

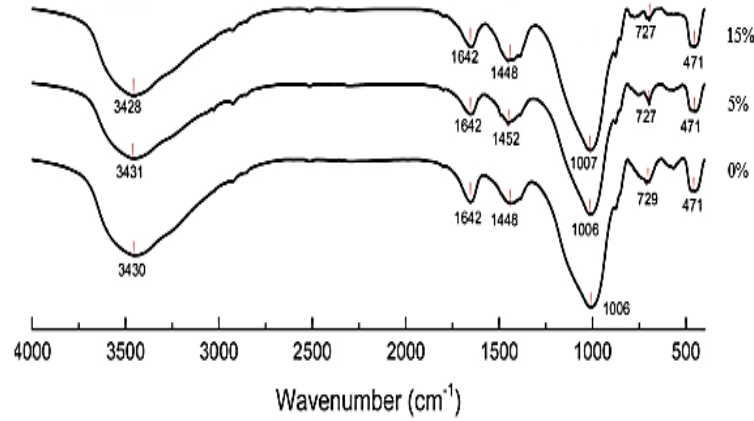


Figure 6. FTIR spectra of geopolymers synthesized with various contents of Oujda Clay.

3.4. TGA Test

Thermogravimetric analysis was conducted on geopolymer concrete samples containing varying amounts of Oujda clay. Powder samples were extracted from the core of geopolymer bricks following a 28-day compressive strength test. All geopolymer samples exhibited similar thermal degradation patterns. Gradual mass loss occurred across all samples with increasing temperature, attributed to moisture loss and changes in the chemical structure of the geopolymer concrete. According to Figure 7, the initial phenomenon observed at 100 °C corresponds to a mass loss due to the evaporation of free and absorbed interstitial water in the geopolymer samples. The condensation can be justified by the disappearance of the band at about 727 cm^{-1} on the IR spectra of geopolymer concrete and geopolymer concrete after heated at 500 °C, indicating further mass loss attributed to the release of structural water and hydroxyl groups from Si–O and Al–O bonds. The total mass loss at this stage was approximately 2% [30].

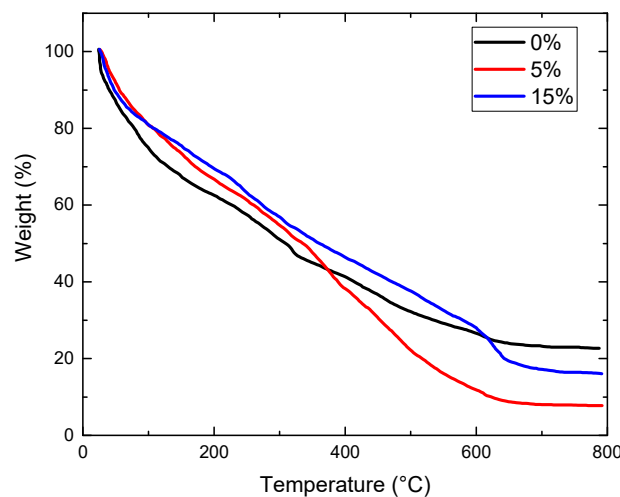


Figure 7. TGA graph of geopolymer samples with various contents of Oujda clay.

3.5. Compressive Strength

The study investigated the compressive strength of geopolymer pastes using varying amounts of Oujda clay replacement, tested after 7 and 28 days of curing. Figure 8 illustrates the results. Increasing the replacement level of Oujda clay (5 to 15 wt%) resulted

in higher compressive strengths at both curing times. Specifically, at 7 days, compressive strength improved from 20.36 to 32.07 MPa. At 28 days, the geopolymer exhibited maximum compressive and flexural strengths when Oujda clay was replaced at 15 wt%, with compressive strength increasing from 21.98 to 33 MPa, and flexural strength from 6 to 10.5 MPa. The high chemical reactivity of Oujda clay enhances the dissolution of aluminosilicate precursors, thereby accelerating the geopolymerization process [31]. One study has shown that crystallization of Na_2SiO_3 and SiO_2 on the surface of geopolymers results in a loss of strength [32]. The increase in the content of Al_2O_3 and SiO_2 improved the geopolymerization and produced the N–A–S–H and C–A–S–H gels, thus enhancing the strength properties of geopolymers [33,34].

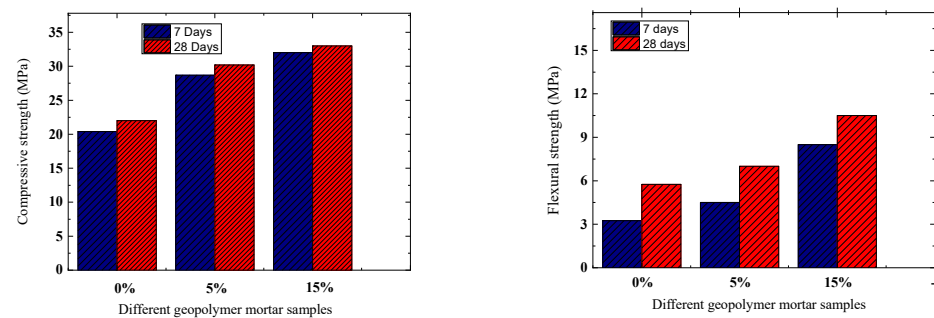


Figure 8. Compressive and flexural strength of different types of geopolymer with various contents of Oujda clay.

4. Conclusions

This study investigated a metakaolin-based geopolymer blended with Oujda clay, replacing 5–15 wt% of MK. Results showed that the Oujda clay addition increased compressive strength to 33 MPa with 15 wt% clay after 28 days of curing. The high chemical activity of Oujda clay accelerated and enhanced the overall performance of the geopolymer. The incorporation of Oujda clay into the metakaolin mix enabled chemical and mechanical properties similar to those of traditional metakaolin-based geopolymers to be maintained, while introducing a locally sourced and potentially more cost-effective material.

Author Contributions: Y.B.: Preparation, investigation, methodology, writing—original draft, review and editing. A.E.: Preparation, investigation, methodology, writing original draft, review and editing. A.T.: Preparation, investigation, methodology, writing original draft, review and editing. All authors have read and agreed to the published version of the manuscript.

Funding: This research received no external funding.

Institutional Review Board Statement: Not applicable.

Informed Consent Statement: Note applicable.

Data Availability Statement: Dataset available on request from the authors.

Conflicts of Interest: The authors declare no conflicts of interest.

References

- Disu, A.A.; Kolay, P.K. A critical appraisal of soil Stabilization using geopolymers: The past, present and future. *Int. J. Geosynth. Gr. Eng.* **2021**, *7*, 23. [\[CrossRef\]](#)
- Duan, P.; Yan, C.; Zhou, W. Compressive strength and microstructure of fly ash based geopolymer blended with silica fume under thermal cycle. *Cem. Concr. Compos.* **2017**, *78*, 108–119. [\[CrossRef\]](#)
- Erfanimesh, A.; Sharbatdar, M.K. Mechanical and microstructural characteristics of geopolymer paste, mortar, and concrete containing local zeolite and slag activated by sodium carbonate. *J. Build. Eng.* **2020**, *32*, 101781. [\[CrossRef\]](#)
- Catauro, M.; Tranquillo, E.; Barrino, F.; Dal Poggetto, G.; Blanco, I.; Cicala, G.; Ognibene, G.; Recca, G. Mechanical and thermal properties of fly ash-filled geopolymers. *J. Therm. Anal. Calorim.* **2019**, *138*, 3267–3276. [\[CrossRef\]](#)
- Topçu, İ.B.; Toprak, M.U.; Uygunoğlu, T. Durability and microstructure characteristics of alkali activated coal bottom ash geopolymer cement. *J. Clean. Prod.* **2014**, *81*, 211–217. [\[CrossRef\]](#)

6. Davidovits, J. Geopolymers: Inorganic polymeric new materials. *J. Therm. Anal. Calorim.* **1991**, *37*, 1633–1656. [[CrossRef](#)]
7. Yang, K.-H.; Song, J.-K.; Song, K.-I. Assessment of CO₂ reduction of alkali-activated concrete. *J. Clean. Prod.* **2013**, *39*, 265–272. [[CrossRef](#)]
8. Dal Poggetto, G.; D'Angelo, A.; Blanco, I.; Piccolella, S.; Leonelli, C.; Catauro, M. FT-IR study, thermal analysis, and evaluation of the antibacterial activity of a MK-geopolymer mortar using glass waste as fine aggregate. *Polymers* **2021**, *13*, 2970. [[CrossRef](#)]
9. Lee, W.-H.; Lin, K.-L.; Chang, T.-H.; Ding, Y.-C.; Cheng, T.-W. Sustainable development and performance evaluation of marble-waste-based geopolymer concrete. *Polymers* **2020**, *12*, 1924. [[CrossRef](#)]
10. Temuujin, J.; Minjigmaa, A.; Rickard, W.; Lee, M.; Williams, I.; Van Riessen, A. Preparation of metakaolin based geopolymer coatings on metal substrates as thermal barriers. *Appl. Clay Sci.* **2009**, *46*, 265–270. [[CrossRef](#)]
11. Görhan, G.; Aslaner, R.; Şinik, O. The effect of curing on the properties of metakaolin and fly ash-based geopolymer paste. *Compos. Part B Eng.* **2016**, *97*, 329–335. [[CrossRef](#)]
12. Li, Z.; Zhang, S.; Zuo, Y.; Chen, W.; Ye, G. Chemical deformation of metakaolin based geopolymer. *Cem. Concr. Res.* **2019**, *120*, 108–118. [[CrossRef](#)]
13. Lecomte, I.; Liégeois, M.; Rulmont, A.; Cloots, R.; Maseri, F. Synthesis and characterization of new inorganic polymeric composites based on kaolin or white clay and on ground-granulated blast furnace slag. *J. Mater. Res.* **2003**, *18*, 2571–2579. [[CrossRef](#)]
14. Rattanasak, U.; Chindaprasirt, P. Influence of NaOH solution on the synthesis of fly ash geopolymer. *Miner. Eng.* **2009**, *22*, 1073–1078. [[CrossRef](#)]
15. Liew, Y.M.; Kamarudin, H.; Al Bakri, A.M.M.; Luqman, M.; Nizar, I.K.; Ruzaidi, C.M.; Heah, C.Y. Processing and characterization of calcined kaolin cement powder. *Constr. Build. Mater.* **2012**, *30*, 794–802. [[CrossRef](#)]
16. Heah, C.Y.; Kamarudin, H.; Al Bakri, A.M.M.; Bnhussain, M.; Luqman, M.; Nizar, I.K.; Ruzaidi, C.M.; Liew, Y.M. Study on solids-to-liquid and alkaline activator ratios on kaolin-based geopolymers. *Constr. Build. Mater.* **2012**, *35*, 912–922. [[CrossRef](#)]
17. Liew, Y.M.; Kamarudin, H.; Al Bakri, A.M.M.; Bnhussain, M.; Luqman, M.; Nizar, I.K.; Ruzaidi, C.M.; Heah, C.Y. Optimization of solids-to-liquid and alkali activator ratios of calcined kaolin geopolymeric powder. *Constr. Build. Mater.* **2012**, *37*, 440–451. [[CrossRef](#)]
18. Cristelo, N.; Glendinning, S.; Teixeira Pinto, A. Deep soft soil improvement by alkaline activation. *Proc. Inst. Civ. Eng. Improv.* **2011**, *164*, 73–82. [[CrossRef](#)]
19. Zhao, Y.X.; Xiang, J.R.; Lü, Q.F.; Shan, X.K.; Chen, Y. Effect of alkali activator on engineering properties of geopolymer-solidified loess. *J. Beijing Univ. Technol.* **2021**, *47*, 637–643.
20. Albidah, A.; Alghannam, M.; Abbas, H.; Almusallam, T.; Al-Salloum, Y. Characteristics of metakaolin-based geopolymer concrete for different mix design parameters. *J. Mater. Res. Technol.* **2021**, *10*, 84–98. [[CrossRef](#)]
21. Churata, R.; Almirón, J.; Vargas, M.; Tupayachy-Quispe, D.; Torres-Almirón, J.; Ortiz-Valdivia, Y.; Velasco, F. Study of Geopolymer Composites Based on Volcanic Ash, Fly Ash, Pozzolan, Metakaolin and Mining Tailing. *Buildings* **2022**, *12*, 1118. [[CrossRef](#)]
22. Nobouassia Bewa, C.; Tchakouté, H.K.; Fotio, D.; Rüscher, C.H.; Kamseu, E.; Leonelli, C. Water resistance and thermal behavior of metakaolin-phosphate-based geopolymer cements. *J. Asian Ceram. Soc.* **2018**, *6*, 271–283. [[CrossRef](#)]
23. Alvarez-Coscojuela, A.; Mañosa, J.; Formosa, J.; Chimenos, J.M. Structural characterisation and reactivity measurement of chemically activated kaolinite. *J. Build. Eng.* **2024**, *87*, 109051. [[CrossRef](#)]
24. Provis, J.L.; van Deventer, J.S.J. Direct measurement of the kinetics of geopolymerisation by in-situ energy dispersive X-ray diffractometry. *J. Mater. Sci.* **2007**, *42*, 2974–2981. [[CrossRef](#)]
25. Davidovits, J. Geopolymers and geopolymeric materials. *J. Therm. Anal.* **1989**, *35*, 429–441. [[CrossRef](#)]
26. Valášková, M.; Klika, Z.; Vlček, J.; Matějová, L.; Topinková, M.; Pálková, H.; Madejová, J. Alkali-activated metakaolins: Mineral chemistry and quantitative mineral composition. *Minerals* **2022**, *12*, 1342. [[CrossRef](#)]
27. Bakharev, T. Resistance of geopolymer materials to acid attack. *Cem. Concr. Res.* **2005**, *35*, 658–670. [[CrossRef](#)]
28. Tchakouté, H.K.; Rüscher, C.H.; Kong, S.; Kamseu, E.; Leonelli, C. Thermal behavior of metakaolin-based geopolymer cements using sodium waterglass from rice husk ash and waste glass as alternative activators. *Waste Biomass Valorization* **2017**, *8*, 573–584. [[CrossRef](#)]
29. Hounsi, A.D.; Lecomte-Nana, G.; Djeteli, G.; Blanchart, P.; Alowanou, D.; Kpelou, P.; Napo, K.; Tchabbedji, G.; Praisler, M. How does Na, K alkali metal concentration change the early age structural characteristic of kaolin-based geopolymers. *Ceram. Int.* **2014**, *40*, 8953–8962. [[CrossRef](#)]
30. Douiri, H.; Kaddoussi, I.; Baklouti, S.; Arous, M.; Fakhfakh, Z. Water molecular dynamics of metakaolin and phosphoric acid-based geopolymers investigated by impedance spectroscopy and DSC/TGA. *J. Non-Cryst. Solids* **2016**, *445*, 95–101. [[CrossRef](#)]
31. Parveen, S.D.; Junaid, M.T.; Jindal, B.B.; Mehta, A. Mechanical and microstructural properties of fly ash based geopolymer concrete incorporating alccofine at ambient curing. *Constr. Build. Mater.* **2018**, *180*, 298–307. [[CrossRef](#)]
32. Alcamand, H.A.; Borges, P.H.R.; Silva, F.A.; Trindade, A.C.C. The effect of matrix composition and calcium content on the sulfate durability of metakaolin and metakaolin/slag alkali-activated mortars. *Ceram. Int.* **2018**, *44*, 5037–5044. [[CrossRef](#)]

33. Huseien, G.F.; Mirza, J.; Ismail, M.; Ghoshal, S.K.; Ariffin, M.A.M. Effect of metakaolin replaced granulated blast furnace slag on fresh and early strength properties of geopolymer mortar. *Ain Shams Eng. J.* **2018**, *9*, 1557–1566. [[CrossRef](#)]
34. Dombrowski, K.; Buchwald, A.; Weil, M. The influence of calcium content on the structure and thermal performance of fly ash based geopolymers. *J. Mater. Sci.* **2007**, *42*, 3033–3043. [[CrossRef](#)]

Disclaimer/Publisher’s Note: The statements, opinions and data contained in all publications are solely those of the individual author(s) and contributor(s) and not of MDPI and/or the editor(s). MDPI and/or the editor(s) disclaim responsibility for any injury to people or property resulting from any ideas, methods, instructions or products referred to in the content.